

**The following resources related to this article are available online at
www.sciencemag.org (this information is current as of October 16, 2009):**

Updated information and services, including high-resolution figures, can be found in the online version of this article at:

<http://www.sciencemag.org/cgi/content/full/315/5818/1544>

Supporting Online Material can be found at:

<http://www.sciencemag.org/cgi/content/full/1136897/DC1>

A list of selected additional articles on the Science Web sites **related to this article** can be found at:

<http://www.sciencemag.org/cgi/content/full/315/5818/1544#related-content>

This article **cites 9 articles**, 1 of which can be accessed for free:

<http://www.sciencemag.org/cgi/content/full/315/5818/1544#otherarticles>

This article has been **cited by** 29 article(s) on the ISI Web of Science.

This article has been **cited by** 3 articles hosted by HighWire Press; see:

<http://www.sciencemag.org/cgi/content/full/315/5818/1544#otherarticles>

This article appears in the following **subject collections**:

Atmospheric Science

<http://www.sciencemag.org/cgi/collection/atmos>

Information about obtaining **reprints** of this article or about obtaining **permission to reproduce this article** in whole or in part can be found at:

<http://www.sciencemag.org/about/permissions.dtl>

An Active Subglacial Water System in West Antarctica Mapped from Space

Helen Amanda Fricker,^{1*} Ted Scambos,² Robert Bindschadler,³ Laurie Padman⁴

Satellite laser altimeter elevation profiles from 2003 to 2006 collected over the lower parts of Whillans and Mercer ice streams, West Antarctica, reveal 14 regions of temporally varying elevation, which we interpret as the surface expression of subglacial water movement. Vertical motion and spatial extent of two of the largest regions are confirmed by satellite image differencing. A major, previously unknown subglacial lake near the grounding line of Whillans Ice Stream is observed to drain 2.0 cubic kilometers of water into the ocean over ~3 years, while elsewhere a similar volume of water is being stored subglacially. These observations reveal a widespread, dynamic subglacial water system that may exert an important control on ice flow and mass balance.

At least 145 subglacial lakes have been mapped beneath the Antarctic Ice Sheet (1). Recent pivotal studies based on satellite data have demonstrated that Antarctic subglacial water can move in large volumes between lakes, on short time scales and over long

distances (2, 3). Large outbursts of subglacial water have been observed in coastal regions (4), but it is not known how frequently these occur, nor the total amount of water involved continent-wide. Water beneath an ice stream, acting as a lubricant either between the ice and subglacial

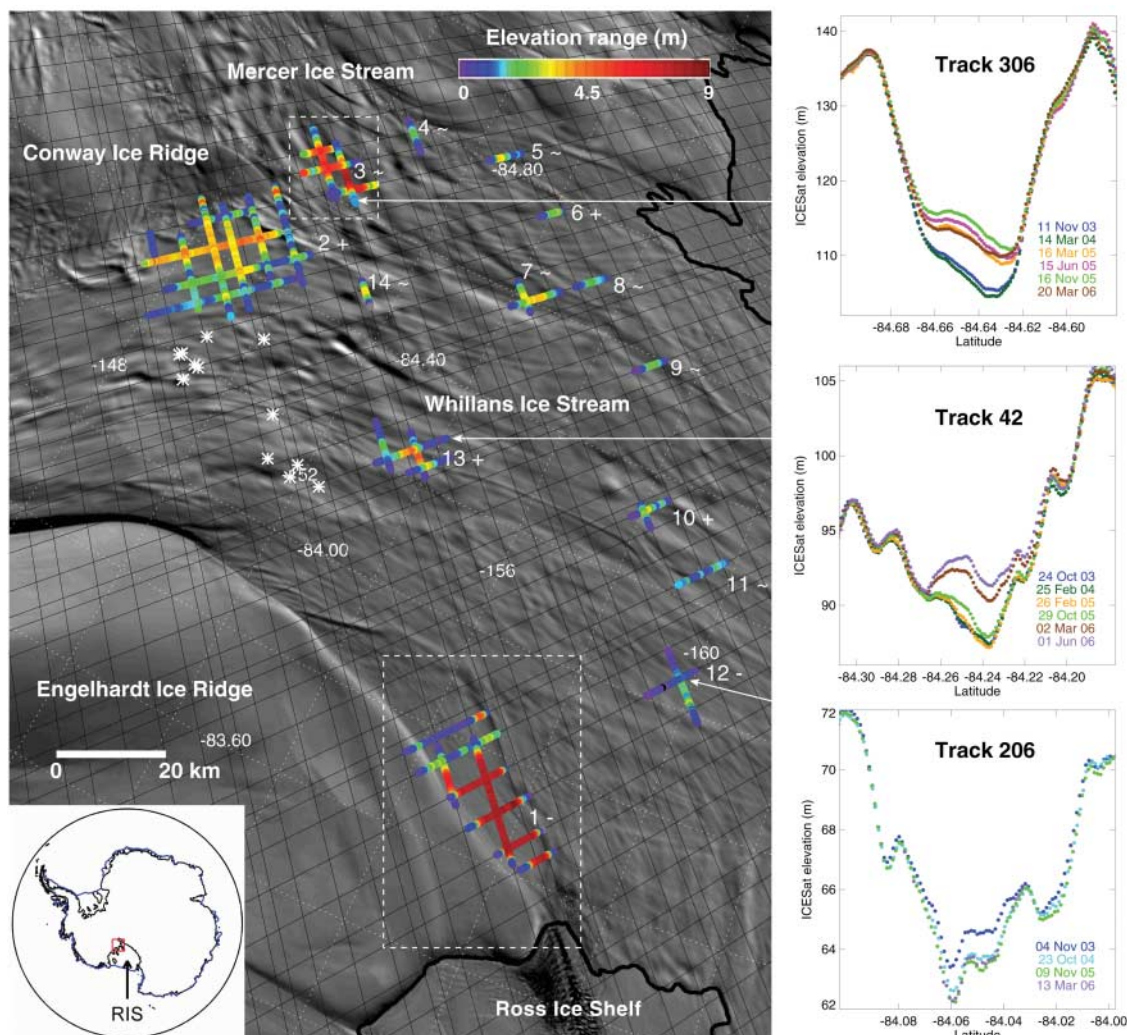
bed or between grains of a subglacial till, affects ice flow rates (5). Subglacial lakes have recently been linked to the broad onset of faster flow of the Recovery Ice Stream (6) and are located at the heads of other Antarctic ice stream tributaries (7). The drastic deceleration (a “shutdown”) ~150 years ago of Kamb Ice Stream has been attributed to a decrease in subglacial water supply (8). Thus, knowledge of subglacial water movement is fundamental to understanding Antarctic ice stream dynamics and to predicting future Antarctic ice sheet behavior and sea-level contribution.

Subglacial water systems are pressurized to near the weight of the overlying ice (9), so movement of water can cause an elevation change of the ice surface that can be detected by satellites. Past observations interpreted to be Antarctic sub-

¹Institute of Geophysics and Planetary Physics, Scripps Institution of Oceanography, University of California, San Diego, La Jolla, CA 92093, USA. ²National Snow and Ice Data Center, University of Colorado, Boulder, CO 80302, USA. ³NASA Goddard Space Flight Center, Greenbelt, MD 20771, USA. ⁴Earth & Space Research, Corvallis, OR 97333, USA.

*To whom correspondence should be addressed. E-mail: hfricker@ucsd.edu

Fig. 1. (Left) Locations of elevation-change events identified through ICESat repeat-track analysis on lower WIS and MIS (2003 to 2006). Straight black lines show the ICESat reference ground tracks. Colored track segments represent range in elevation amplitude for each elevation-change event. Events cluster into 14 elevation-change regions, which are either rising (+), falling (−), or oscillating (−). Ice flow is from top left to lower right. Background image is MODIS Mosaic of Antarctica (MOA) (30), and inset map shows its location in Antarctica. Bold black line indicates the break-in-slope associated with the grounding zone of the Ross Ice Shelf (RIS). White dashed boxes show regions covered in Fig. 2. White asterisks indicate locations of small surface-collapse features observed on WIS in 1987–1988 (fig. S4). **(Right)** Repeat ICESat elevation profiles along track segments that cross each type of region (−, +, −). Arrows point to the location of each track segment on the image.



glacial water movement have been made with interferometric synthetic aperture radar (InSAR) (2) and satellite radar altimetry (3). However, InSAR data for high southern latitudes ($>80^{\circ}\text{S}$) are presently limited to a brief period during late 1997 (10, 11). Radar altimetry has a relatively long record and many repeat observations, but has limited coverage and spatial resolution (12).

ICESat Laser Altimetry

Our approach combines accurate, repeated elevation profiling from satellite laser altimetry with satellite image differencing to map and monitor elevation changes. NASA's Ice, Cloud, and land Elevation Satellite (ICESat), which carries the Geoscience Laser Altimeter

System (GLAS), provides elevation data with a small (~ 65 m) spatial footprint, high vertical accuracy [± 20 cm (13)], and high along-track resolution (~ 170 m). We analyzed all available ICESat data across the Whillans and Mercer ice streams (WIS and MIS) (Fig. 1) from a series of 10 data-acquisition periods spanning February 2003 through June 2006 (Table 1) for apparent elevation changes using repeat-track analysis (14, 15). This indicated 101 candidate elevation-change "events." Horizontal offsets of repeated tracks (up to ~ 500 m) cause apparent elevation changes in the presence of nonzero cross-track slopes. To focus on temporal variability, we conservatively discarded events where the elevation trend was correlated with track offset. Most

of the 46 remaining events showed a change in elevation confined to a trough or basin bounded by steeper sections of the ice stream surface (Fig. 1). Plotting these events on an image map showed that they clustered in 14 distinct elevation-change regions in the vicinity of the WIS/MIS confluence and grounding line (Fig. 1). Events within each region had consistent patterns of timing and displacement magnitude. The large (~ 350 km²) region, near the grounding line of Ross Ice Shelf (RIS) next to Engelhardt Ice Ridge (near the bottom of Fig. 1), has the largest-amplitude signal and is a special case that will be discussed later. The other two large regions are located on either side of Conway Ridge; one on WIS (~ 500 km²) and the other on MIS (~ 120 km²). The remaining elevation-change regions in the lower glacier trunk are smaller, being sampled by just one to four tracks, and sum to an estimated area of 250 km². None are identified over the central trunk of WIS between 148°W and 140°W , but there are five additional smaller-amplitude regions farther upstream (fig. S1). Some events may be undetectable with our technique and conservative criteria, especially in the central ice stream where topography is rougher. Overall, $\sim 10\%$ of the lower WIS/MIS area shown in Fig. 1 is occupied by elevation-change regions. The smallest along-track extent of the 46 events was 3.5 km and the mean extent was 9.1 km, suggesting that ICESat track spacing in this area (3 to 5 km) (Fig. 1) is adequate to capture most changing regions.

Table 1. ICESat operations periods, orbit repeat periods, dates of data acquisition, and release numbers (46) for the data used in this work. ICESat has operated in two repeat orbits: 8 and 91 days, the latter with a 33-day subcycle. The last 33 days of the Laser 2a 91-day operations period (since 10/25/2003) have been repeated in all subsequent operations periods (Laser 2b onward) ~ 4 months apart.

Operations period	Repeat (days)	Dates	Release
Laser 1	8	02/20/03–03/29/03	118
Laser 2a	8	09/25/03–10/04/03	426
Laser 2a	91	10/04/03–11/19/03	426
Laser 2b	91	02/17/04–03/21/04	428
Laser 2c	91	05/18/04–06/21/04	117
Laser 3a	91	10/03/04–11/08/04	428
Laser 3b	91	02/17/05–03/24/05	428
Laser 3c	91	05/20/05–06/23/05	122
Laser 3d	91	10/21/05–11/24/05	428
Laser 3e	91	02/22/06–03/28/06	428
Laser 3f	91	05/24/06–06/26/06	126

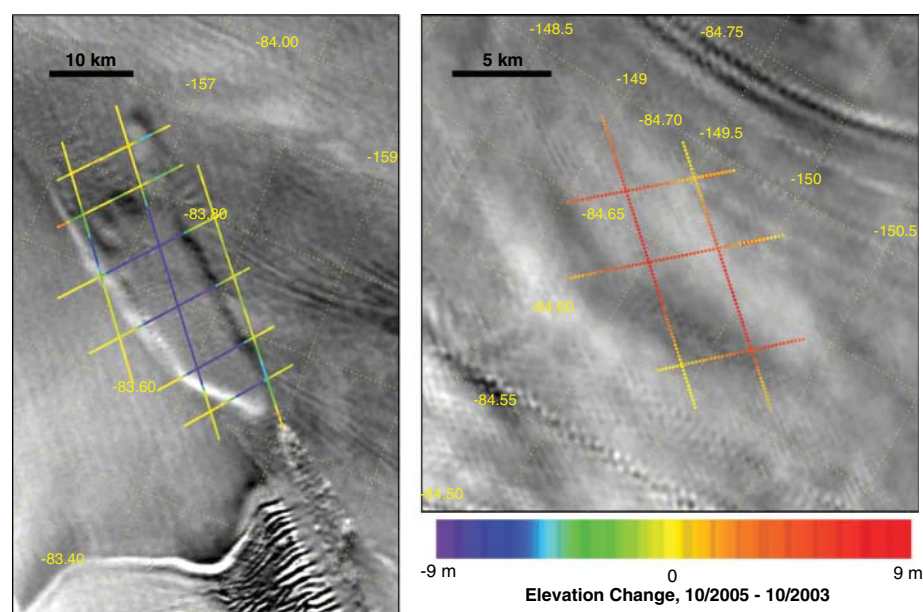


Fig. 2. MODIS difference images (December 2005 minus December 2003) over regions 1 (left) and 3 (right). ICESat tracks across both regions are color-coded by the elevation change from October/November 2003 to October/November 2005, close in time to when the images that were differenced were acquired. Illumination of all images used to make the difference images was from the upper right. Images for region 1 are shown as an animated sequence in movie S2.

Satellite Image Differencing

To map the spatial extent of the elevation-change regions and to confirm the ICESat-detected changes, we used a technique involving subtraction of similarly illuminated groups of satellite images. High-precision radiometric images of a uniform snow/ice surface are sensitive to surface slope (16, 17). We used images from the Moderate-resolution Imaging Spectroradiometer (MODIS) sensor, flying on NASA's Terra and Aqua satellites. We constructed a multiyear series of calibrated surface reflectance images from multiple cloud-masked, destriped, visible-band scenes acquired over brief intervals (a few weeks) each year (fig. S2). This "image stacking" process yields scenes with improved radiometric and spatial detail (18). By subtracting these images, the resultant image emphasizes areas where surface slope changed [see "Satellite Image Differencing" in (19)]. Figure 2 illustrates how image differencing complements the ICESat analysis by defining the spatial extent of the two regions with the largest elevation changes. For these regions, image differencing confirmed the sign of surface elevation change and the relative magnitude of the surface slope changes. No additional regions of change were identified.

Interpretation

The detected elevation-change regions display a variety of temporal signatures. The three largest regions show nearly constant activity between

each ICESat operation period, whereas other regions were frequently quiescent. The track segments undergoing change between ICESat operation periods were nearly constant. Transects of elevation differences (not shown) for small regions were approximately Gaussian in shape, whereas tracks across the larger regions (1 and 2 in Fig. 1) had flat central portions with the differences decreasing toward each end. The constancy of the spatial extent during growth or decay, the short time scale of the changes, the shape of the flexural boundaries (14), and the locations of the changes (in basins) are all consistent with water-driven elevation change, and not consistent with the sudden formation or erosion of subglacial landforms as recently reported beneath another Antarctic ice stream (20). We interpret these elevation-change regions as surface expressions of ponded subglacial water, and the observed surface movement to be due to water gain or loss through a system of conduits beneath the ice streams. This concept is visualized in movie S1. We have detected similar signals on MacAyeal Ice Stream (fig. S3). We refer to regions 1, 2, 3, and 13 as subglacial lakes Engelhardt, Conway, Mercer, and Whillans, respectively, based on nearby named ice features.

Using ice-thickness data (21) and a smoothed digital elevation model from ICESat data (22), we mapped the hydraulic potential [or subglacial pressure field; see “Calculation of hydraulic potential pressure” in (19)] and compared it with the distribution of inferred active subglacial water locations (Fig. 3). Resolution of our pressure map is 7.5 km. Errors in the estimated potential are ± 10 kPa of the mean at this averaging scale, but larger (~ 100 kPa) localized variations may be associated with smaller-scale surface or bed topography. Relative minima in the subglacial pressure field identify areas that would tend to collect and retain water; steep pressure gradients promote rapid water movement; and the direction of subglacial water flow is toward lower pressure and normal to equipotential contours. Several of the identified elevation changes, including subglacial lakes Whillans, Mercer, and Engelhardt, coincide with lows in the regional subglacial pressure, while Subglacial Lake Conway is in an area of low potential gradient.

Although existence of a subglacial water system long has been suspected beneath active West Antarctic ice streams (5, 8), the present observation of rapid movement between several reservoirs is unprecedented. The only direct evidence of pooled subglacial water comes from drilling in the upstream portion of Kamb Ice Stream (23). Indirect evidence comes from InSAR (2), seismic data (24), and airborne observations of small collapse features on WIS in 1987–1988 (Fig. 1 and fig. S4). Although they are close by, these locations do not coincide with features identified here. WIS and MIS are fast-flowing ice streams and have a soft till layer at their beds (25). Given the recent observation that large volumes of sediment can be transported rapidly beneath ice

streams (20), it is possible that on longer time scales (decades to centuries), the features we have identified may migrate. A large bottom crevasse, at least 12 km long, detected at the base of WIS (26) by radio-echo sounding may have been the expression of a conduit that formed part of the subglacial system at that time.

Subglacial Lake Engelhardt Drainage Event

ICESat observations. The observed drainage of Subglacial Lake Engelhardt is particularly noteworthy. Figure 4 shows sequential elevation profiles for two ICESat tracks across the lake and the elevation evolution at three cross-overs (27). The first ICESat profile across the lake was acquired in February 2003 (Laser 1), along a track of an 8-day repeat-orbit configuration that was almost coincident with Track 206 from the 91-day repeat-orbit configuration used

for all observations from October 2003 onward (Fig. 1). Between October 2003 and November 2005, elevations decreased by ~ 9 m at a gradually decreasing rate over most of the basin, while maintaining the flat surface shape in the region's center. Drainage ceased after November 2005. The ICESat data have sufficient along-track resolution to reveal the expected ice flexure at the lake margins during drainage (28). ICESat data acquired during 2006 suggest that some uplift has occurred, indicative of slow refilling of the lake (29).

Image differencing. Annual difference images spanning the period 2000 to 2005 are consistent with drainage starting in 2003 and continuing through 2005 (Fig. 2 and fig. S2). The images also confirm the flat surface shape in the center during deflation and the flexure at the edges, and reveal several elongated areas

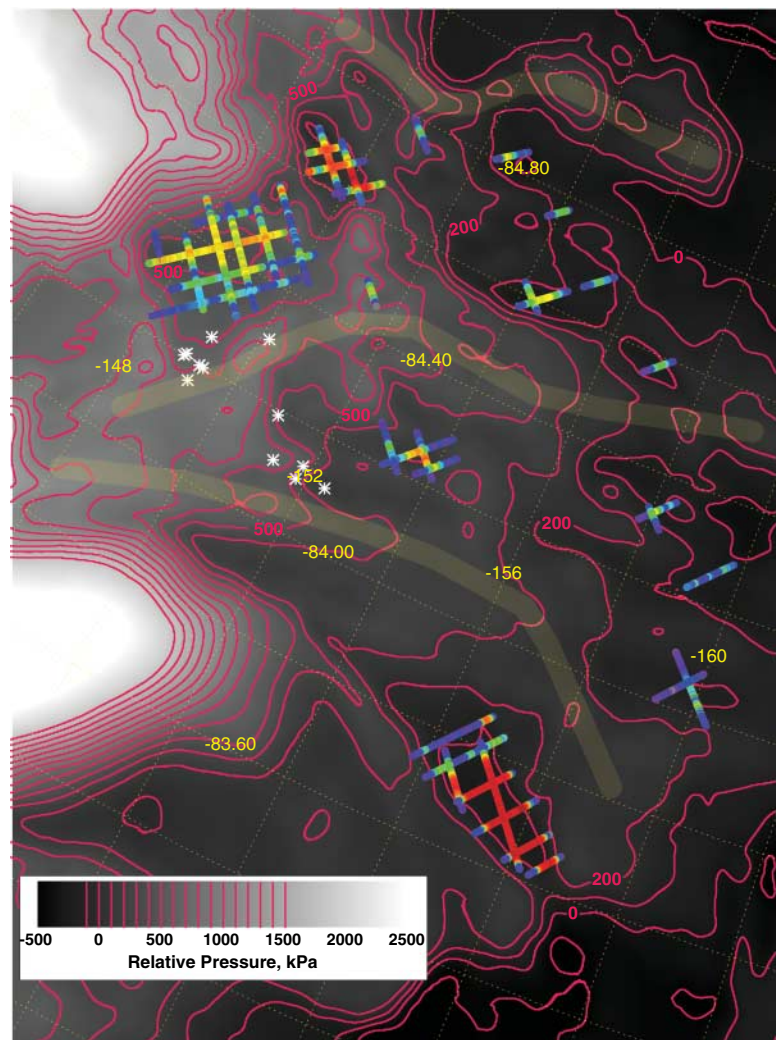


Fig. 3. Inferred subglacial water (hydrostatic) pressure at the base of the ice, in kilopascals (kPa), relative to the value at the grounding line near Subglacial Lake Engelhardt. The pressure-field resolution is ~ 7.5 km [see “Calculation of hydraulic potential pressure” in (19)]. Contours (interval 100 kPa) and gray-scale both represent hydrostatic pressure (dark indicates lower pressure). The broad yellow bars highlight “ridges” in the pressure field that may separate subglacial drainages. Figure covers the same area as Fig. 1, and colored track values represent range in elevation amplitude as in Fig. 1. White asterisks indicate locations of small surface-collapse features observed on WIS in 1987–1988 (fig. S4).

near the region's upstream end. They also show that the downstream end of the feature is ~ 7 km from the grounding line of the Ross Ice Shelf as mapped by both surface slope change in MODIS imagery (30) and ICESat repeat-track analysis (14). The outline of the basin is marked by the increasing slope at its edges (Fig. 4 profiles), and ICESat profile locations of greatest change fit precisely within the boundary of the basin as defined by the imagery.

Hydraulic path, discharge rate, and total volume lost. The hydraulic path for the Subglacial Lake Engelhardt water was across the grounding line into the ocean. The subglacial pressure field (Fig. 3) shows that lake pressure was likely 100 to 200 kPa higher than the pressure of the ocean at the grounding line before drainage (31). The downstream end of the lake is closed off from the ocean by a weak pressure barrier of ~ 50 kPa. This was presumably breached during drainage by a conduit too small

to be resolved in the potential map. Based on the subsidence area and the elevation decrease, the lake lost ~ 2.0 km³ of water to the ocean cavity beneath RIS. The initial maximum rate of 1.25 km³ year⁻¹ (~ 40 m³ s⁻¹) was sustained for 18 months. For comparison, jökulhlaups (outbursts of subglacially stored water) typically reach discharge rates one to two orders of magnitude larger but only last for days (32). The relatively low pressure differential (33) may explain the absence of an exponential growth in the discharge typical of jökulhlaups, leading to the observed more gradual drainage at a nearly constant rate. We cannot determine from the data the dimensions of the outlet conduit (34), nor whether it consisted of a single channel either in the ice or the subglacial till (35), a flowing water sheet (36), or a network of linked channels. Previous authors (3) inferred a steady flow rate for a subglacial lake in East Antarctica (37), which they attributed to a modification of the overburden pressure as

the ice roof deformed to accommodate the changing water volumes. For Lake Engelhardt drainage, flexure is limited to a narrow (~ 1 km) zone at the margin, and little energy was expended to deform the roof (38); therefore, the roof subsidence must have kept pace with the drainage. Termination of discharge may have occurred because the declining pressure head could no longer overcome closure of the outlet path, or the lake had achieved hydraulic equilibrium with the adjacent sub-ice-shelf cavity. We see no evidence of a tidal response of the lake since discharge ceased.

Lake history and possible trigger mechanism. We examined historic data sets (both field and satellite) to assess prior states of Subglacial Lake Engelhardt and found no evidence of prior drainage (supporting online text). The 2003–2006 drainage event may have been triggered by a longer-term ice thinning and local upstream migration of the grounding line (39), causing the lake seal (ice dam) to break. This thinning and migration of the grounding zone can be seen in fig. S2 and movie S2. We calculated migration rates of 443 ± 60 m year⁻¹ and 330 ± 100 m year⁻¹ from ICESat (2003 to 2006) and MODIS (2000 to 2005), respectively.

Hydraulic Linkage and Volume Estimate for Water Within the WIS/MIS System

The subglacial hydraulic pressure field beneath the ice streams (Fig. 3) includes three major divides that control water flow direction and separate regions of subglacial water activity (40). More than half of the subglacial area of WIS is hydraulically directed toward Subglacial Lake Conway. Drainage from this subglacial reservoir appears to be directed southward into Subglacial Lake Mercer and, from there, westward to spread more broadly across the ice plain. ICESat's temporal records of elevation change in this catchment support our interpretation; Subglacial Lake Mercer and regions 4 and 5 (Fig. 1) all indicate water loss between late 2005 and mid-2006, whereas the four regions downstream (6, 7, 8, and 9) grow by an amount equal to half of their combined drained volume. Subglacial Lake Whillans lies in a more restricted catchment that narrows upstream. It was relatively quiescent until a sudden surface inflation began in late 2005 at a rate of ~ 8 m year⁻¹. Regions 10, 11, and 12 downstream are active throughout the ICESat measurement period, with a small net gain in volume. The third catchment feeds Subglacial Lake Engelhardt and is confined to the northern margin of WIS by the northernmost divide in the pressure field.

We have shown that Subglacial Lake Engelhardt drained during the first 2.7 years of the ICESat mission, with a total volume loss of ~ 2.0 km³. In the same period, Subglacial Lake Conway steadily filled, with a total volume increase of 1.2 km³. The surface of Subglacial Lake Mercer oscillated, rising between 2003 and late 2005 (see Track 306 on Fig. 1, and Fig. 2) and sinking from late 2005 to mid-2006, for a net volume gain of 0.12 km³. The remaining

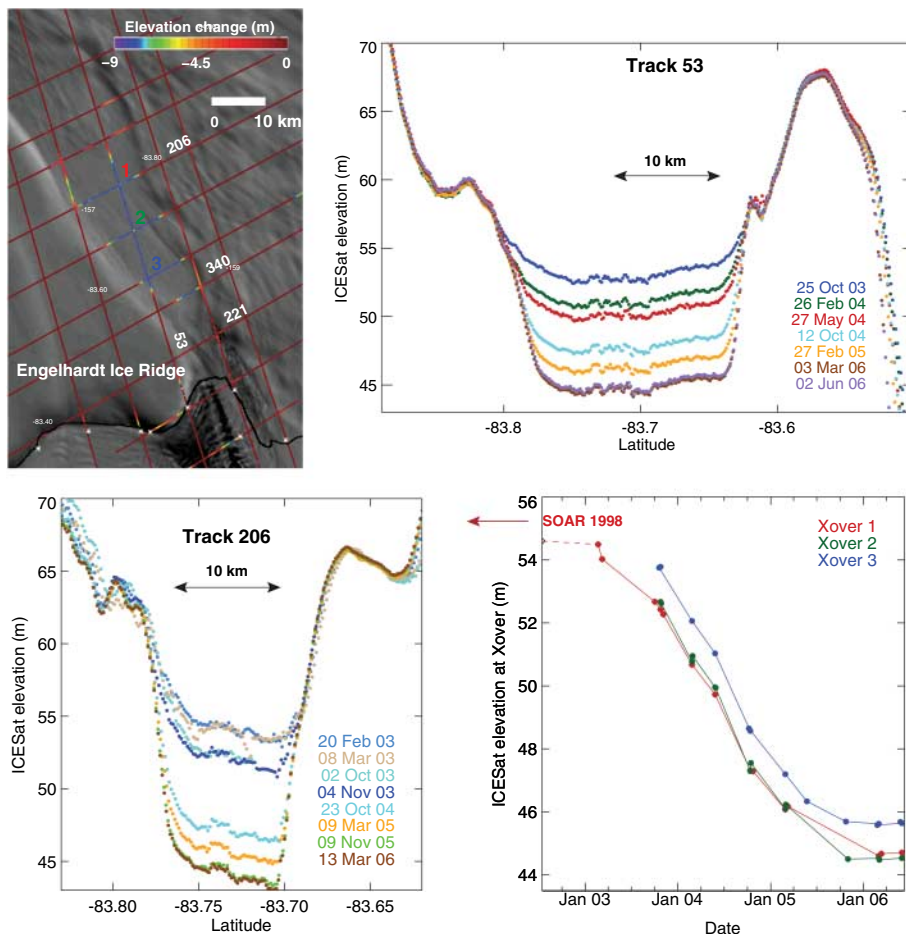


Fig. 4. (Top left) ICESat 91-day tracks across newly discovered Subglacial Lake Engelhardt on northwestern WIS. Background image is MOA (30). Tracks are color-coded by elevation change between October 2003 and November 2005. White asterisks locate tide-induced ice-flexure limits for the grounding line derived from ICESat repeat-track analysis (14). (Top right and bottom left) Repeat ICESat profiles along two tracks across the lake (see top left panel for locations). Track 206 was an almost exact repeat of an 8-day track, and the first three profiles were acquired in this orbit (Laser 1 and Laser 2; Table 1). (Bottom right) ICESat elevations against time at three orbit crossovers in the center of the lake (see top left panel for locations), including the 8-day data at crossover 1 in February/March 2003. SOAR data from 1998 (indicated by an arrow) are discussed in the supporting online material.

elevation-change areas summed to a total volume increase of 0.27 km^3 , but we found little temporal coherence between them. Ignoring the few regions far upstream on WIS and the isolated Subglacial Lake Engelhardt, the incremental water stored during each interval between ICESat observations (~ 4 months) varied from $+0.05$ to $+0.4 \text{ km}^3$. The total volume increase was 1.6 km^3 summed over 33 months (or $\sim 0.6 \text{ km}^3 \text{ year}^{-1}$), which is approximately equal to the volume of water lost from Subglacial Lake Engelhardt (2.0 km^3). The average annual rate of water storage is similar to the estimated area-integrated production rate for basal water ($0.53 \text{ km}^3 \text{ year}^{-1}$) over the entire $168,000\text{-km}^2$ catchment of WIS (41). Thus, a substantial fraction of the subglacial water produced beneath these ice streams transits through the observed subglacial water system. The volume of fresh water injected into the ocean cavity under the RIS is small relative to the net production from basal melt under the RIS, but may influence the thermohaline circulation in the sub-ice-shelf cavity close to the source.

Net storage of water in the system, sustained from one ICESat observation interval to the next, is not an equilibrium situation: Eventually the water must either freeze onto the base of the ice stream or be discharged, perhaps in the manner we observed for Subglacial Lake Engelhardt. Because that lake lost as much volume as was gained elsewhere, the net change in water volume in the whole system for 2003 to 2006 was close to zero. However, the subglacial catchment map shows that it is not the same water; Subglacial Lake Engelhardt is not hydraulically linked to any of the other observed lakes in the system. Present basal conditions of WIS and MIS promote basal freezing (41), probably inhibiting water discharge and possibly explaining the current tendency to store subglacial water. Additionally, tidally modulated stick-slip motion [which results in twice-daily transitions between rapid ice flow and nearly no ice flow (42)], observed over most of the lower part of WIS, may interfere with the movement of subglacial water on a daily basis. Water will flow toward isolated low-pressure regions, which are preferentially located in the types of local surface depressions we identify as collecting subglacial water. As water accumulates, as it is presently doing in Subglacial Lake Conway, the hydrostatic pressure will eventually overcome the glaciostatic pressure leading to lake discharge (32), and the water will drain either to another basin or across the grounding line into the ocean. This cycle of draining and filling may influence the ice stream velocity, on short time scales of weeks to months. Variability of subglacial water production and storage may explain the recent slowdown of WIS (43, 44).

Summary

Repeat-track ICESat laser altimetry, with complementary image differencing, provides a new, effective technique for monitoring water movement under glacial ice. Using this approach, we

have discovered a widespread, active water system underneath the Whillans and Mercer ice streams, two of the largest streams draining the West Antarctic Ice Sheet. The detected motions are large, extensive, and temporally variable. They suggest that there is a net gain in water over the observation interval (2003 to 2006), which is likely both reflecting and influencing the motion of these major Antarctic ice streams. These observations provide clues to understanding the stability of ice streams through their sensitivity to basal lubrication. The time scale for subglacial water transport (months to years) is short compared with that of other known drivers of glacial flow variability, suggesting a mechanism for more rapid changes in ice stream behavior than have previously been assumed.

References and Notes

1. M. Siegert, S. Carter, I. Tabacco, S. Popov, D. Blankenship, *Antarct. Sci.* **17**, 453 (2005).
2. L. Gray *et al.*, *Geophys. Res. Lett.* **32**, L03501 (2005).
3. D. J. Wingham, M. L. Siegert, A. Shepherd, A. S. Muir, *Nature* **440**, 1033 (2006).
4. I. Goodwin, *J. Glaciol.* **34**, 95 (1988).
5. B. Kamb, *Antarct. Res. Ser.* **77**, 157 (2001).
6. R. E. Bell, M. Studinger, C. A. Shuman, M. A. Fahnestock, I. Joughin, *Nature* **445**, 904 (2007).
7. M. Siegert, J. Bamber, *J. Glaciol.* **46**, 703 (2000).
8. R. B. Alley, S. Anandakrishnan, C. R. Bentley, N. Lord, *Ann. Glaciol.* **20**, 187 (1994).
9. A. Iken, R. A. Bindschadler, *J. Glaciol.* **32**, 101 (1986).
10. The three-dimensional InSAR technique requires ascending and descending passes, which only exist in a few areas of Antarctica. InSAR data for Antarctica are mainly derived from the tandem mission of European Remote-sensing Satellite-1 (ERS-1) and ERS-2 (18 months in 1995–1996). RADARSAT provided InSAR data as far as the South Pole, but only for 3 months in 1997 (9).
11. K. C. Jezek, *Ann. Glaciol.* **29**, 286 (1999).
12. U.S. Navy's GEOSAT operated to 72°S during 1985 to 1989 in a 17-day orbit; the European Space Agency has flown three radar altimeters (RAs) in a 35-day orbit to 81.5°S : ERS-1 (1991 to 2000); ERS-2 (1995 to 2003); and Envisat (2002 to present). All four of these satellites miss much of the dynamic West Antarctic ice streams. The RA has a large footprint (~ 2 to 3 km over flat ice for ERS). Steep slopes on the ice streams cause tracking problems for the RA, limiting its vertical accuracy.
13. C. A. Shuman *et al.*, *Geophys. Res. Lett.* **33**, L07501 (2006).
14. H. A. Fricker, L. Padman, *Geophys. Res. Lett.* **33**, L15502 (2006).
15. ICESat data were filtered for clouds by use of the gain and energy parameters. Elevation anomalies for each segment were calculated by resampling the remaining repeat-track data onto common latitude values and calculating the difference between each elevation profile and the mean. At each point, the elevation range was also calculated.
16. T. A. Scambos, G. Kvaran, M. Fahnestock, *Remote Sens. Environ.* **69**, 56 (1999).
17. R. A. Bindschadler, P. L. Vornberger, *Ann. Glaciol.* **20**, 327 (1994).
18. T. A. Scambos, M. A. Fahnestock, *J. Glaciol.* **44**, 97 (1998).
19. Materials and methods are available as supporting material on Science Online.
20. A. M. Smith *et al.*, *Geology* **35**, 127 (2007).
21. S. Shabtaie, C. R. Bentley, *Ann. Glaciol.* **11**, 126 (1988).
22. J. DiMarzio, J. Zwally, A. Brenner, B. Schutz, Boulder, Colorado, USA: National Snow and Ice Data Center. Digital media (2007).
23. S. W. Vogel *et al.*, *Geophys. Res. Lett.* **32**, L14502 (2005).
24. S. R. Atre, C. R. Bentley, *Ann. Glaciol.* **20**, 177 (1994).
25. D. D. Blankenship, C. R. Bentley, S. T. Rooney, R. B. Alley, *J. Geophys. Res.* **92**, 8903 (1987).
26. C. R. Bentley, R. Retzlaff, N. Lord, A. N. Novick, *Antarct. J. U.S.* **26**, 62 (1991).

27. In satellite altimetry data, crossover analysis is a powerful means to validate elevation along any single track (45) and is the method previously used to detect subglacial water movement in ERS RA data (3).
28. G. W. Evatt, A. C. Fowler, C. D. Clark, N. R. J. Hulton, *Philos. Trans. R. Soc. A* **364**, 1769 (2006).
29. The latest ICESat data shown in Fig. 4 (Laser 3f data; May to June 2006) suggest that minor uplift occurred, but at levels close to the ICESat detection limit. Initial examination of data from the most recent operations period (Laser 3g, November to December 2006) suggests that this filling has continued, but since those data are still uncalibrated for precise pointing, we cannot yet confidently assert that the signal is real.
30. T. A. Scambos, T. Haran, M. A. Fahnestock, T. Painter, J. Bohlander, *Remote Sens. Environ.*, in press.
31. This estimate is in part affected by some surface lowering that had already taken place at the epoch of ICESat's Laser 2a data, which were used to create the digital elevation model.
32. M. J. Roberts, *Rev. Geophys.* **43**, RG1002 (2005).
33. A pressure of 100 kPa corresponds to a 10-m vertical difference in water-column height.
34. From the MODIS imagery (Figs. 2 and 4), we observe that the shortest length for a channel connecting the lake to the ocean is $\sim 7 \text{ km}$ long. ICESat data along Track 221 show a depression $\sim 2 \text{ km}$ wide, which gives an upper bound to the width of the outlet channel.
35. H. Rothlisberger, *J. Glaciol.* **11**, 177 (1972).
36. G. E. Flowers, H. Björnsson, F. Pálsson, G. K. C. Clarke, *Geophys. Res. Lett.* **31**, L05401 (2004).
37. The discharge curve we observe is similar to that for Lake L1 in (3). The drop in elevation is $\sim 9 \text{ m}$ for Lake Engelhardt compared to $\sim 3.5 \text{ m}$ for Lake L1, and the time scale is 26 months for Lake Engelhardt compared to 16 months for Lake L1.
38. The dimensions of Subglacial Lake Engelhardt are $\sim 30 \text{ km}$ by $\sim 10 \text{ km}$, i.e., 14 to 40 times the ice thickness ($\sim 700 \text{ m}$), so the central ice cannot be supported at the lake margins. The flat surface profiles in the center of the lake confirm this.
39. R. Bindschadler, P. Vornberger, *Science* **279**, 689 (1998).
40. Errors in the surface-elevation and ice-thickness fields used for subglacial pressure mapping could modify the subglacial water catchments and allow some exchange of water between them. These issues were examined by adding $\pm 5\text{-m}$ and $\pm 50\text{-m}$ random errors to the surface and bed elevations, respectively. The major features discussed here did not change.
41. I. Joughin, S. Tulaczyk, D. R. MacAyeal, H. Englehardt, *J. Glaciol.* **50**, 96 (2004).
42. R. A. Bindschadler, M. King, R. A. Alley, S. Anandakrishnan, L. Padman, *Science* **301**, 1087 (2003).
43. R. Bindschadler, P. Vornberger, L. Gray, *J. Glaciol.* **51**, 620 (2005).
44. I. Joughin *et al.*, *Geophys. Res. Lett.* **32**, L22501 (2005).
45. H. J. Zwally, R. A. Bindschadler, A. C. Brenner, T. V. Martin, R. H. Thomas, *J. Geophys. Res.* **88**, 1589 (1983).
46. ICESat data release numbers are of the form YXX. Y refers to the amount of orbit and attitude calibration applied (a good indicator of quality), where 1 is the lowest and 4 is the highest. XX refers to the software version used to process the data.
47. We thank K. Yanagimachi, C. Bentley, D. Blankenship, J. Bohlander, G. Clarke, N. Lord, B. Smith, and D. Young for their contributions to this work. Thanks to J. Zwally, B. Schutz, and NASA's ICESat project. Thanks also to two anonymous referees for helpful comments on this manuscript. This work was supported by NASA. This is ESR contribution number 86.

Supporting Online Material

www.sciencemag.org/cgi/content/full/1136897/DC1
Materials and Methods
SOM Text
Figs. S1 to S4
References
Movies S1 and S2

30 October 2006; accepted 8 February 2007
Published online 15 February 2007;
10.1126/science.1136897
Include this information when citing this paper.